Poly(vinyl alcohol) Reinforced and Toughened with Poly(dopamine)-Treated Graphene Oxide, and Its Use for Humidity Sensing

Sang-Ha Hwang,[†,‡,∥] Dongwoo Kang,[†,§,∥] Rodney S. Ruoff,[⊥] Hyeon Suk Shin,[†,§,*] and Young-Bin Park[†,‡,*]

[†]Low Dimensional Carbon Materials Center, [‡]School of Mechanical and Nuclear Engineering, [§]School of Natural Science, and [⊥]Center for Multidimensional Carbon Materials, Institute of Basic Sciences, Ulsan National Institute of Science and Technology, UNIST-gil 50, Eonyang-eup, Ulju-gun, Ulsan 689-798 Republic of Korea. [∥]S.-H. Hwang and D. Kang were equal major contributors to this work.

ABSTRACT Poly(dopamine)-treated graphene oxide/poly(vinyl alcohol) ("dG-O/PVA") composite films were made and characterized. G-O was modified with poly(dopamine) in aqueous solution and then chemically reduced to yield poly(dopamine)-treated reduced G-O. A combination of hydrogen bonding, strong adhesion of poly(dopamine) at the interface of PVA and G-O sheets, and reinforcement by G-O resulted in increases in tensile modulus, ultimate tensile strength, and strain-to-failure by 39, 100, and 89%, respectively, at 0.5 wt % dG-O loading of the PVA. The dG-O serves as a moisture barrier for water-soluble PVA, and the dG-O/PVA composite films were shown to be effective humidity sensors over the relative humidity range 40−100%.

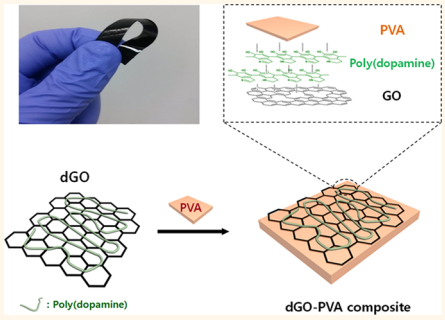

KEYWORDS: graphene oxide · poly(dopamine) · nanocomposite · interfacial adhesion · reinforcement · toughening · humidity sensing

Carbon/polymer nanostructure composites have been studied in part due to the possibility of achieving superior mechanical, electrical, and optical properties.[1−3] Carbon nanotubes (CNTs) have been widely used as a filler in polymer matrices, but agglomeration, the presence of catalytic impurities, and relatively high cost have presented challenges. Chemically modified graphene has been studied as a new type of filler[4−7] due in part to its potential for imparting excellent mechanical, electrical, and optical properties in polymer composites.[3,8,9]

Graphene oxide (G-O), *i.e.*, single layers of graphite oxide, can be obtained through simple dispersion in water, and because such individual layers can be readily achieved, it has been of interest to use chemically modified graphene as a filler in composite materials.[10−12] Oxygen-containing functional groups, including hydroxyl, epoxide, ketone, and carboxylic acid, render G-O water-dispersible.[12−14] In certain cases, such functional groups may improve the interfacial bonding to the matrix as has been reported for some functionalized CNTs.[15] Polymer composites containing functionalized graphene are a relatively new area of composites research.[3] Some studies have indicated significant improvements in composite properties, with the degree of dispersion of the functionalized graphene in the polymer matrix reported as particularly important.[16,17] In some studies exceptional improvements were reported for very low filler loadings, and this was ascribed to the large surface area of graphene-based fillers.[9,18]

In addition to G-O and related functionalized graphene sheets, expanded graphite and exfoliated graphite "nanoplatelets" have also been used as fillers to make conducting composites, sometimes also with improved mechanical, thermal, and optical properties. There have been many studies of polymer composites made with expanded or exfoliated graphite including epoxy, poly(methyl methacrylate) (PMMA), polypropylene, linear low density polyethylene (LLDPE), high density polyethylene

* Address correspondence to shin@unist.ac.kr, ypark@unist.ac.kr.

Received for review January 25, 2014 and accepted June 9, 2014.

Published online June 09, 2014
10.1021/nn500504s

(HDPE), polystyrene, polyphenylene sulfide (PPS), nylon, and silicone rubber.[19−25] These studies reported that expanded or exfoliated graphite as a filler can increase tensile modulus by 8−130%; ultimate tensile strength, however, is reported in some studies to be increased and in others to be decreased. Stankovich *et al.*[9] reported the preparation of chemically functionalized graphene/polymer composites and an electrical percolation threshold of only 0.1 vol %, specifically with polystyrene. Ramanathan *et al.*[26] studied the mechanical properties of chemically functionalized graphene sheet/PMMA composites and reported substantially improved interaction between the host polymer and the chemically functionalized graphene compared to those containing expanded/exfoliated graphite or unmodified single-walled carbon nanotubes.

Oxygen-containing functional groups are reported to be well suited for composites with a polar polymer matrix, such as PMMA, polyacrylonitrile (PAN) and poly(acrylic acid) (PAA), and "intimate" graphene/polymer interactions and a percolated interphase essential for mechanical enhancement have been reported.[26] Therefore, poly(vinyl alcohol) PVA filled with, *e.g.*, G-O, could be a good combination for achieving strong interfacial bonding, as PVA chains should strongly bind on the surface of G-O by hydrogen bonding. On the basis of this rationale, PVA/G-O composites have been explored both experimentally and theoretically, and the relationship between hydrogen bonding density and the mechanical properties of the composites has been studied. Zhang *et al.*[27] and Wang *et al.*[28] reported increased tensile modulus, strength, and strain-to-failure at G-O loadings lower than 1−1.8 wt %. Wang *et al.* reported that the yield strengths of G-O/PVA composites increased linearly up to 11.01 MPa (a 136% increase compared to neat PVA) as G-O content was increased from 0 to 5 wt %; a maximum strain-to-failure of 210% (a 27% increase) was reported at 1.5 wt % loading. Chemically functionalized graphene sheets covalently bonded to PVA were studied, and yield strength and strain-to-failure of 72 MPa and 191%, respectively, were reported at 0.5 wt % loading.[28] Zhang *et al.*, reported tensile strength and strain-to-failure of 3.48 MPa (a 132% increase) and 165% (a 62% increase) at 1 wt % loading for the same composite system. G-O/PVA or chemically functionalized graphene/PVA composites are reported to show this unusual increase in toughness because of their "molecular level" dispersion and high density of hydrogen bonding. An ideal configuration would be when the edges of the sheets are joined together side by side. However, when a critical content is reached, *i.e.*, 1−1.8 wt %, the G-O sheets begin to stack together driven by the strong van der Waals force, decreasing the efficiency of the mechanical reinforcement.[27]

Dopamine, which is a small molecule containing catechol and amine groups, is a kind of hormone and

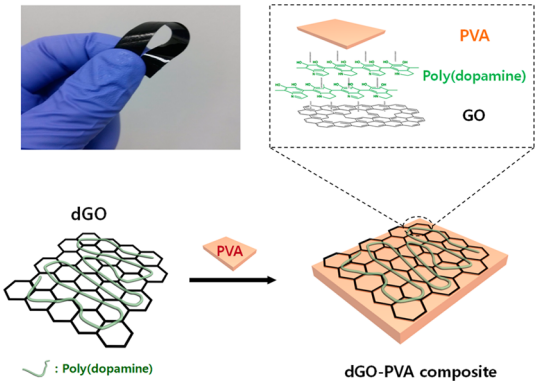

Figure 1. A photograph and proposed structure of a dG-O/PVA composite film.

neurotransmitter, and its polymerized form, known as poly(dopamine), is similar to adhesive proteins of mussels. At a weak alkaline pH condition, dopamine self-polymerizes to produce an adherent poly(dopamine) coating on a wide range of substrates[29−31] with the oxidation of catechol groups to the quinone form. It binds strongly to most organic and inorganic surfaces, such as metals, metal oxides, and polymer surfaces. Also, the oxidized quinone form of catechol can undergo reactions with various functional groups, such as thiol, amine, and quinone itself, by Michael addition or the Schiff base reaction to form covalently grafted functional layers. Moreover, dopamine could be used to reduce G-O during its polymerization on the G-O surface.[32]

Here, we report a simple and practical approach to synthesize graphene-reinforced PVA composite films by combining graphene oxide (G-O) with poly(dopamine), (dG-O), in an aqueous solution with the simultaneous reduction of G-O to reduced graphene oxide sheets. The dG-O/PVA composites obtained exhibited significant improvements in mechanical properties as a result of increased interfacial interactions produced by the combined mechanisms of hydrogen bonding between amine and hydroxyl groups of poly(dopamine) and abundant hydroxyl groups of PVA and polymer entanglement between PVA and poly(dopamine) (Figure 1).[33] Poly(dopamine) is also believed to play a role of binding with G-O sheets *via* hydrogen bonding between amine and hydroxyl groups of poly(dopamine) and hydroxyl groups of G-O as well as $\pi-\pi$ of G-O interaction between catechol and small graphitic domains of G-O.[34] With the addition of dG-O, we achieved simultaneous improvements in tensile modulus, strength, and strain-to-failure. We also demonstrated that dG-O/PVA composite films can be used as structurally robust humidity sensors that use electrical conductivity to measure humidity.

RESULTS AND DISCUSSION

Characterization of dG-O. dG-O was prepared by mixing an aqueous suspension of graphene oxide (G-O)

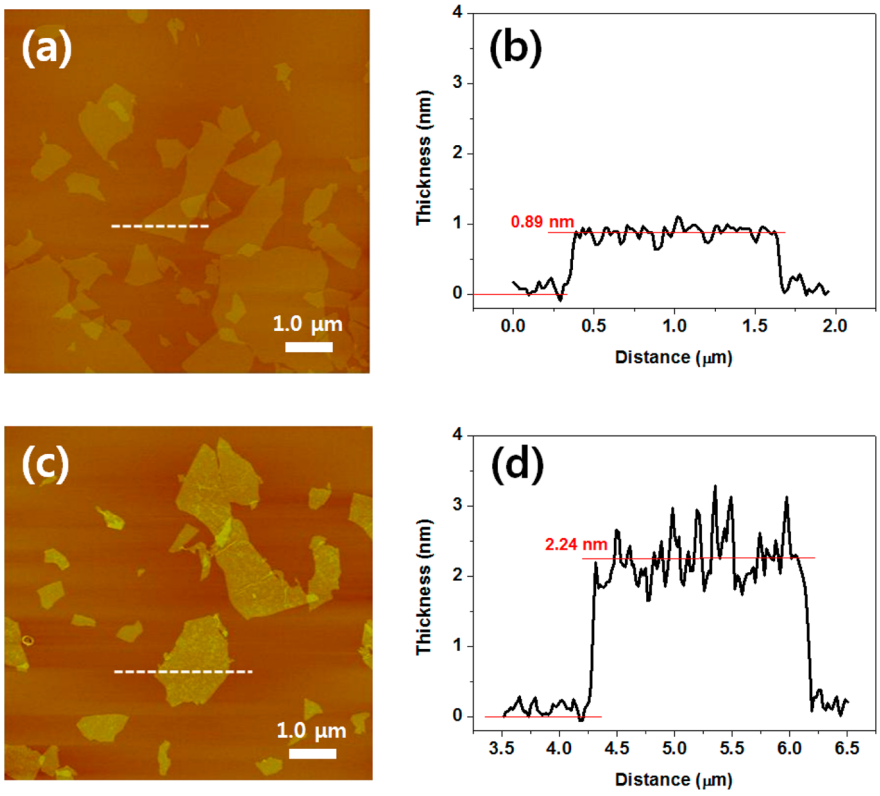

Figure 2. (a,b) AFM image and height profile of G-O. (c,d) AFM image and height profile of dG-O. G-O and dG-O (dopamine:-G-O = 0.5:1) samples were spin-coated on a Si wafer for AFM measurements.

and a solution of dopamine hydrochloride in a buffer solution (10 mM Tris-HCl, pH 8.5). In a basic aqueous solution, poly(dopamine) is spontaneously formed by oxidative polymerization. The solutions were prepared with different G-O/poly(dopamine) ratios such as 0.25:1, 0.5:1, and 1:1 (w/w). It was confirmed from scanning electron microscopy (SEM) images that the dG-O sheets were well-dispersed in deionized water. The increase in thickness of the G-O sheets by coating them with poly-(dopamine) was determined by atomic force microscopy (AFM). Figure 2 shows the morphology and thickness of G-O and dG-O sheets. The thickness of as-prepared G-O sheets was around 0.89 nm, which is thicker than pristine graphene due to the functional groups on the graphene surfaces produced by the oxidation (Figure 2(a,b)).[35,36] On the other hand, the average thickness of dG-O was around 2.24 nm (Figure 2(c,d)), indicating that the increase in thickness of 1.35 nm is due to the presence of poly(dopamine) on the G-O sheets. Note that poly-(dopamine) has a very similar structure to eumelanin, which is characterized by an interconnected layered structure along the *z*-axis with a graphite-like stacking spacing of 3.4−3.8 Å.[37−40]

The poly(dopamine) coating on the G-O sheets was also proved by X-ray photoelectron spectroscopy (XPS). XPS survey spectra of G-O and dG-O samples in Figure 3(a) showed that a N 1s peak at 398 eV was observed in only the dG-O sample. The N 1s peak originates from amine groups of the poly(dopamine) layer on G-O sheets. From the XPS spectrum of the dG-O sample, the nitrogen/carbon atomic ratio (N/C) was calculated to be 0.095 (Table S1, Supporting Information). It has been reported that the theoretical value of N/C in dopamine is 0.125 and the N/C value in poly(dopamine) layers on different substrates is between 0.1and 0.13.[29] So, if we consider the G-O layer as a substrate, the N/C value of 0.095 in our sample is quite reasonable. Figure 3(b) shows that in the C 1s binding region a peak due to oxygen-containing groups between 286 and 290 eV in the G-O sample has been mostly removed in the dG-O sample, indicating partial reduction of G-O by the adsorption and polymerization of dopamine. Indeed, it has been known that G-O can be reduced by released electrons during oxidative polymerization of catecholeamines such as dopamine and norepinephrine.[41]

We measured attenuated total reflectance Fourier transform infrared (ATR-FTIR) spectra of G-O and dG-O as shown in Figure 4.The typical FTIR spectrum of G-O shows O−H stretching vibrations in the region of 3000 to 3400 cm^{-1}, C═O stretching vibrations from carbonyl and carboxylic groups at 1720 cm^{-1}, skeletal vibrations from unoxidized graphitic domains at 1620 cm^{-1}, C−OH stretching vibrations at 1160 cm^{-1},and C−O stretching vibrations at 1040 cm^{-1}.[35,42] On the other hand, the FT-IR spectrum of the dG-O sample showed a newly developed peak at 1500 cm^{-1}, corresponding to the N−H bending mode of aromatic secondary amine in dG-O.[43] This result confirms that the poly(dopamine)

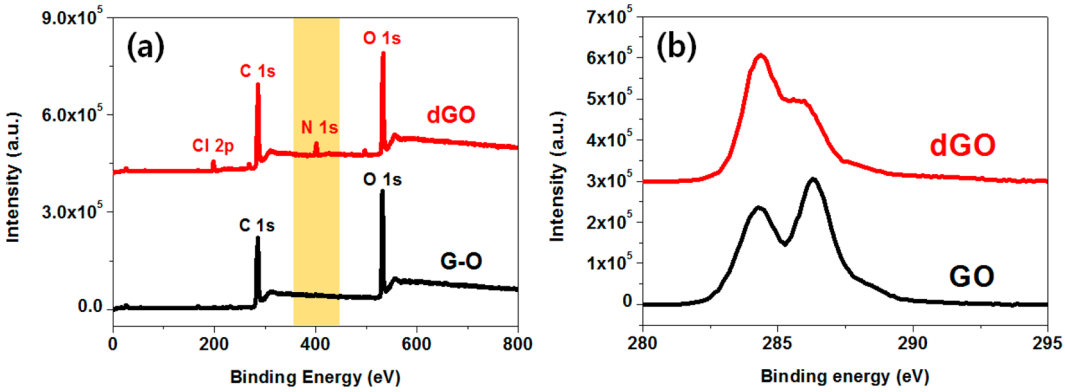

Figure 3. (a) XPS survey spectra and (b) C 1s binding energy region of G-O and dG-O spin-coated on a Si wafer. An additional Cl 2p peak in (a) originates from dopamine hydrochloride (HCl), which was used as the precursor of poly(dopamine).

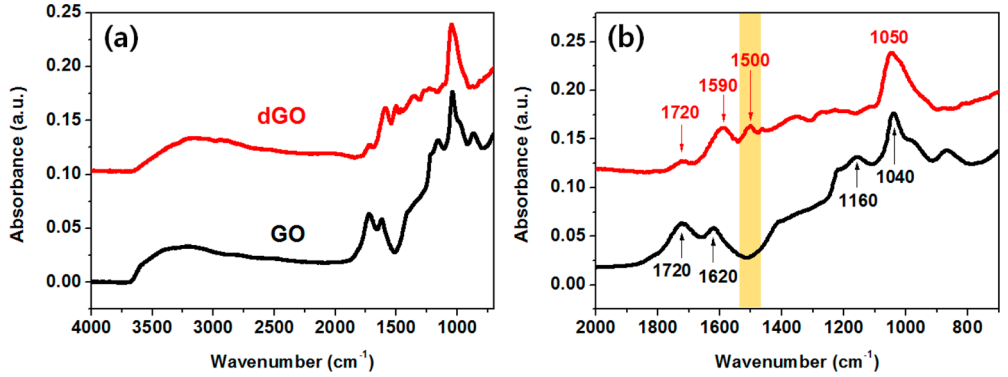

Figure 4. (a) ATR-FTIR spectra of G-O and dG-O samples in the region between 4000 and 700 cm^{-1} and (b) magnified wavenumber range of 2000 to 700 cm^{-1} of G-O and dG-O. To obtain a thick film of G-O and dG-O for ATR-FTIR measurement, each solution was repeatedly coated onto a Si wafer by drop casting.

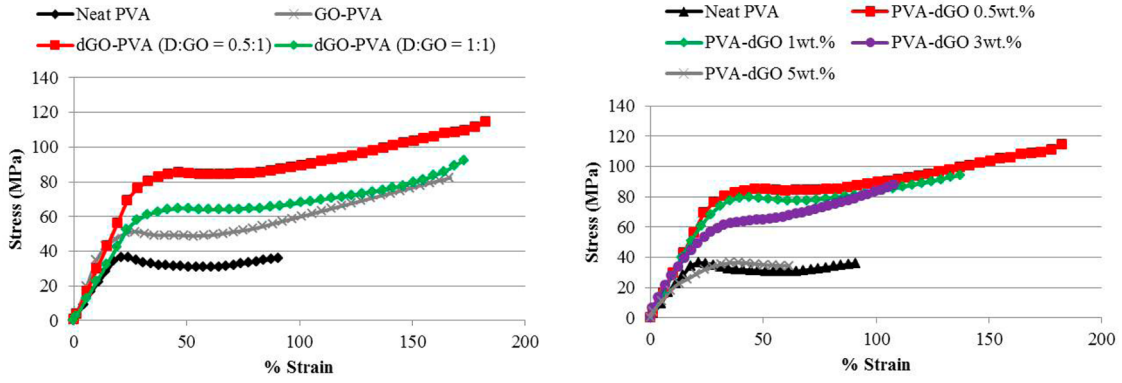

Figure 5. Stress−strain curves of (a) neat PVA, G-O/PVA, dG-O/PVA composite films at 0.5 wt % G-O or dG-O loading and (b) dG-O/PVA composite films with various dG-O loadings (poly(dopamine):G-O = 0.5:1).

on the G-O sheets possesses aromatic, nitrogenous species, such as the indole- or indoline- type structures widely proposed in poly(dopamine) and eumelanins.[37] Note that the region between 3000 and 3400 cm^{-1} could not be used to identify the N−H stretching mode of secondary amine due to the broad band in the region possibly caused by strong hydrogen bonds between poly(dopamine) and oxygen-containing groups in G-O sheets.

Mechanical Properties of dG-O/PVA Films. The mechanical properties of a composite reflect the state of its homogeneity and the interfacial interactions between its constituents. Typical stress−strain behaviors of dG-O/PVA composites with different poly(dopamine):G-O ratios and dG-O contents are shown in Figure 5(a,b) and summarized in Tables 1 and 2. Previous research confirmed that G-O has a significant effect on the mechanical properties of PVA composites.[3−5] In particular, Wang *et al.*[28] showed that PVA is toughened by G-O and rG-O at very low loadings (~0.5 wt %). Figure 5(a) shows both reinforcement and toughening.

TABLE 1. Tensile Properties of G-O/PVA and dG-O/PVA Composites (at 0.5 wt % G-O Loading)

film type	neat PVA	G-O/PVA	dG-O/PVA (D:G-O = 0.5:1)	dG-O/PVA (D:G-O = 1:1)
E(GPa)	2.10	3.31	2.92	2.48
UTS (MPa)	41.48	53.37	82.92	62.47
strain-to-failure (%)	97.15	161.28	183.68	172.75

TABLE 2. Tensile Properties of dG-O/PVA Composites (Poly(dopamine):G-O = 0.5:1)

dG-O content (wt %)	0	0.5	1	3	5
E(GPa)	2.10	2.92	3.12	3.34	1.95
UTS (MPa)	41.48	82.92	80.92	80.92	39.12
strain-to-failure (%)	97.15	183.68	132.51	119.95	52.82

From Table 1, the average tensile modulus increases from 2.1 GPa for neat PVA to 3.31 GPa for a 0.5 wt % G-O/PVA composite. In addition, the tensile strength also increases from 41.48 to 53.37 MPa, and the maximum strain-to-failure increases from 97.15 to 161.28%.

It is obvious that dG-O is a more effective reinforcement for PVA compared to as-synthesized G-O. Table 1 shows that the addition of 0.5 wt % dG-O to poly(dopamine):G-O with a weight ratio of 0.5:1 results in the highest tensile strength of 82.9 MPa and a strain-to-failure of 184%. At a poly(dopamine):G-O ratio of 1:1, the mechanical properties of the material were slightly decreased compared to that for the 0.5:1 ratio; however, they were still higher than the those of the as-prepared G-O/PVA composite at the same loading. As the amount of poly(dopamine) layer becomes "excessive," the heterogeneity between poly(dopamine) and PVA begins to generate a miscibility issue, thus adversely affecting the interfacial bonding and load transfer.

Figure 5(b) and Table 2 show that when dG-O content in poly(dopamine):G-O = 0.5:1 increases above 0.5 wt %, the ultimate tensile strength and maximum strain-to-failure decrease while the tensile modulus increases. This may be attributed to the fact that at dG-O contents above 0.5 wt %, dG-O restacking begins to dominate over the reinforcing effect, which adversely affects these parameters. As described by Wang *et al.*,[28] several possible arrangements are available for graphene nanosheets in the polymer matrix, among which side-by-side joining represents the ideal condition. When a critical content is reached, graphene sheets begin to restack together as the distance between two sheets become so small and the van der Waals force becomes substantial.[44] On the other hand, the tensile modulus increases because it is more dependent on the wt % of dG-O and is much less sensitive to interfacial bonding.

Water Resistance of dG-O/PVA Films. To measure the effect of dG-O on the swelling behavior of PVA films, water uptake of the composite films was measured as a function of time. As shown in Figure 6(a), the general observation is that all the samples show a relatively drastic increase in water adsorption up to ~5 h, where it begins to level off. It is evident that the extent of water uptake decreases with increasing dG-O content, indicative of dG-O serving as a moisture barrier. G-O is hydrophilic and contains numerous hydroxyl groups, which accelerate water adsorption when exposed to moisture. However, G-O provides nanodispersed sites whose interactions with the surrounding PVA molecules restrain the swelling of G-O/PVA composites, leading to a lower swelling ratio. Zhang *et al.*[27] reported a critical maximum swelling ratio of ~170% at 0.6 wt % G-O. However, our dG-O/PVA composites show a lower maximum swelling ratio (around 120% at 3 or 5 wt % dG-O) compared to a neat PVA film. Hence, it is believed that strong adhesion of poly(dopamine) to PVA chains can prevent swelling of the composites. Thus, a larger interfacial area was physically cross-linked by dG-O in PVA films as shown in Figure 1. Also, water-dipping tests for the composite films in Figure 6(b,c) show interesting results in that composites with 3 and 5 wt % of dG-O exhibited no weight loss after 12 h, whereas the neat PVA film dissolved in water and essentially disappeared.

Humidity Sensing Performance of dG-O/PVA Composite Films. PVA films with a dG-O filler can serve as an effective humidity sensor due to their ability to absorb moisture to a moderate level while maintaining their structural integrity, with dG-O serving as a moisture barrier as shown in Figure 6. The swelling of the polymer matrix due to moisture absorption leads to an increase in electrical resistance as the electrical conductive network formed by dG-O nanosheets becomes disrupted.

Electrical resistance *versus* RH is plotted for 3 and 5 wt % dG-O/PVA films in Figure 7(a) and (b). On the basis of the compositions of the composites, the mechanism behind the change in resistance when subjected to humidity can be explained as follows. In dG-O/PVA composites, PVA acts as an insulating matrix. Meanwhile, polymerization of poly(dopamine) facilitates partial chemical reduction of G-O, which imparts electrical conductivity in dG-O/PVA composite films. When the surface of a dG-O/PVA film is exposed to water molecules, adsorption occurs and capillary condensation of water produces a proton (H^+) as shown in eq 1.

$$H_2O = H^+ + OH^- \quad (1)$$

This proton can be a carrier for the improvement of electrical conduction in dG-O/PVA films, and more protons are produced when the sensing material is exposed to more humidity in the testing system.[45] In Figure 7(a), the resistance of dG-O/PVA films is plotted

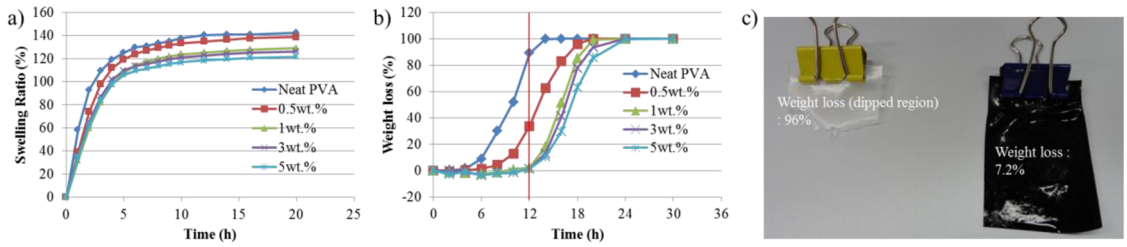

Figure 6. (a) Swelling ratio, (b) weight losses measured from water-dipping tests performed on dried dG-O/PVA (poly(dopamine):G-O = 0.5:1) composite films with various G-O contents. (c) Optical photograph shows difference in weight loss between neat PVA and dG-O/PVA films after 12 h of dipping in water at room temperature.

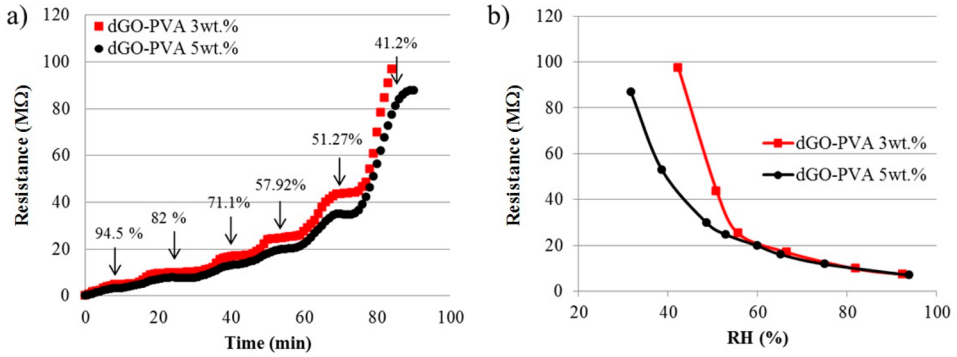

Figure 7. Variation of resistance with respect to (a) stepwise dehumidification and (b) linear humidification for different dG-O loadings.

with stepwise dehumidification from a RH of 94.5 to 41.2%. From a comparison of 3 and 5 wt % dG-O/PVA composite films, it is clear that the 3 wt % film shows a more drastic increase in resistance below 50% RH. This is attributed to the fact that at 3 wt % the loosely interconnected dG-O conductive network is more susceptible to proton removal by dehumidification, compared to the 5 wt % material. In both stepwise dehumidification and continuous humidification cases, nonlinear resistance changes with respect to RH were observed, and the samples were more moisture-sensitive at lower RH values. This may be due to the fact that proton saturation for conduction is more readily reached in low-humidity regions and is in good agreement with other reported results from PVA-based humidity sensors.[46,47]

To characterize the repeatability and response of dG-O/PVA films, dynamic adsorption−desorption cycles between 40 and 60% RH were used. Figure 8 shows the time response and recovery curve of a 5 wt % dG-O/PVA film subjected to humidification-dehumidification cycles with a period of 10 min. The sample showed excellent sensing repeatability, and the difference in maximum resistance was less than 1% over 4 cycles. It is expected that the humidity sensing repeatability under cyclic input will be valid outside the range of 40−60% RH, although the sensitivity will be lower above 60% RH.

Barkauskas[48] showed the extremely narrow humidity sensing range of PVA (between 98 and 99% RH, or 1.17% ΔRH) could be widened to 43.4% ΔRH by using

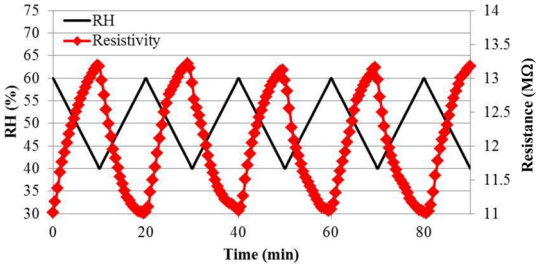

Figure 8. Resistance reversibility in the response of a 5 wt % dG-O/PVA film at 30 °C.

different substrates, aging and the addition of carbon black. To overcome this issue of a limited sensing range, Li *et al.*[46] used polyaniline as a main sensor material, which was combined with PVA for water absorption. Yang *et al.*[49] added electrolytes, such as sodium chloride (NaCl) to a PVA matrix to increase both the sensitivity and sensitivity range of the PVA films. Both approaches suffer from limitations in long-term stability and mechanical properties because of electrolyte loss and oxidation. However, we broadened the sensitivity range of PVA-based humidity sensors to 58.3% ΔRH without sacrificing structural integrity and long-term performance.

CONCLUSIONS

A simple approach was used to produce G-O modified with poly(dopamine) in aqueous solution followed by spontaneous reduction of G-O during the polymerization of dopamine to yield dG-O. A combination of

hydrogen bonding, strong adhesion of poly(dopamine) at the interface of PVA and G-O, and reinforcing effects of G-O resulted in simultaneous increases in tensile modulus, ultimate tensile strength, and strain-to-failure of 39, 100, and 89%, respectively, at a 0.5 wt % dG-O loading. It was also demonstrated that dG-O can serve as an effective moisture barrier in inherently water-soluble PVA and enables dG-O/PVA composite films to be used as robust, cost-effective, easy-to-use humidity sensors over the relative humidity range of 40−100%. It was shown that the dG-O concentration in PVA, which governs proton generation, can serve as an effective parameter to control the moisture sensitivity and that the composite films are robust under cyclic humidification-dehumidification conditions. Although PVA is a water-soluble polymer and, therefore, its detectable humidity range is quite narrow, the addition of a small amount of dG-O, which acts as an effective moisture barrier, can extend the sensing range significantly, prolong the continuous sensing time, and improve the physical stability with a reduction in moisture-induced aging.

METHODS

Materials. Graphite (SP-1, Bay Carbon), H_2SO_4 (98%, Merck), P_2O_5 (99.99%, Aldrich), $K_2S_2O_8$ (99.0%, Sigma-Aldrich), $KMnO_4$ (99.0%, Sigma-Aldrich), H_2O_2 (30%, Daejung), dopamine hydrochloride (98.5%, Sigma) and tris-HCl (99.9%, Baker) were used as received without further purification.

Preparation of Graphene Oxide (G-O) Solution. Graphite oxide was prepared from purified natural graphite (SP-1, Bay Carbon) using the modified Hummers method. The graphite powder (2.0 g) was put into a solution of concentrated H_2SO_4 (3.0 mL), $K_2S_2O_8$ (1.0 g), and P_2O_5 (1.0 g) at 80 °C. The resultant dark blue mixture was allowed to cool to room temperature over a period of 6 h and was then carefully diluted with distilled water, filtered, and washed on the filter until the pH of the rinsewater became neutral. The product was dried in air at ambient conditions overnight. This preoxidized graphite was then subjected to oxidation by the Hummers method. The preoxidized graphite powder (2.0 g) was added to concentrated H_2SO_4 (46 mL) and $KMnO_4$ (6.0 g) was added gradually with stirring and cooling, while the temperature of the mixture was maintained below 20 °C. The mixture was then stirred at 35 °C for 2 h, and distilled water (92 mL) was added. After 15 min, the reaction was terminated by the addition of a large amount of distilled water (280 mL) and a 30% H_2O_2 solution (5.0 mL), after which the color of the mixture changed from black to bright yellow. The mixture was filtered and washed with a 1:10 HCl solution (500 mL) in order to remove metal ions. The graphite oxide product was suspended in distilled water to give a viscous, brown dispersion, which was subjected to dialysis to completely remove metal ions and acids. To obtain the G-O dispersion, graphite oxide was exfoliated by treatment with a mechanical homogenizer at 15 000 rpm for 15 min, followed by sonication (ultrasonic cleaner, 100 W, Branson) for 15 min and then centrifugation at 4000 rpm for 10 min.

Preparation of dG-O Solution. 75 mg of dopamine hydrochloride was added into a 150 mL tris-HCl buffer solution (10 mM), and pH of the solution was tuned to 8.5 using 0.1 M NaOH solution. Then, this solution was mixed with 150 mL of the G-O suspension (1.0 mg/mL) at ambient conditions and the mixture stirred for 2 h at room temperature. Finally, the color of the solution turned to dark brown due to the pH-induced oxidative polymerization of dopamine hydrochloride and the reduction of G-O.

Fabrication of dG-O/PVA Composite Films. The fabrication procedure for the dG-O/PVA composite (G-O loading = 0.5 wt %) was as follows: dG-O was dispersed in distilled water (15 mL) in an ultrasonic bath for 60 min at room temperature. PVA (~2 g) was dissolved in distilled water (200 mL) at 90 °C. After the PVA-H_2O solution had cooled to around 60 °C, the dG-O aqueous dispersion was gradually poured into the PVA solution and sonicated for an additional 15 min at room temperature. Finally, this homogeneous dG-O/PVA solution was poured into a Teflon Petri dish and kept at 60 °C for film formation until its weight equilibrated. The film was peeled from the substrate and was hot pressed at 200 °C in order to eliminate any remaining voids. A series of dG-O/PVA composite films with various poly(dopamine): G-O ratios (1:0, 0.5:1, 1:1) was similarly prepared. In all these samples, the G-O content was kept constant at 0.5 wt %. For comparison, G-O/PVA composite films were prepared according to the same procedure with a loading of 0.5 wt %. As a reference sample, a pure PVA film was prepared by the hot casting technique.

Characterization of dG-O/PVA Composite Films. Tensile properties, including modulus, strength, and strain-to-failure, of the films fabricated were measured using a dynamical mechanical analyzer (DMA Q800, TA Instruments), operated under a quasi-static, strain-controlled mode at a constant strain rate of 20%/min. Specimens measuring 45 mm by 12 mm with a thickness of 80 μm were laser-cut (VersaLaser VLS2.30, Universal Laser Systems) and installed in a film tensile fixture. Tensile tests were performed until the specimens ruptured. Load and elongation were measured simultaneously. The morphology of the fracture surfaces of tensile specimens was analyzed using a scanning electron microscope (SEM, FEI Nanonova 230).

To assess the potential applicability of dG-O/PVA composite films as humidity sensors, water uptake, quantified by swelling ratio, and humidity sensitivity were measured. Vacuum-dried film samples were immersed in distilled water until saturated and their weight became constant. The samples were then removed from the water, and their surfaces were blotted with a filter paper before being weighed. The swelling ratios of the films were calculated using the following formula:

$$\text{swelling ratio} = \frac{W - W_0}{W_0} \times 100(\%) \qquad (2)$$

where W_0 and W are the weights of the sample before and after immersing in water, respectively.

A strip of a dG-O/PVA composite film was installed in an in-house-fabricated fixture devised to measure humidity sensitivity (Figure S2, Supporting Information). The fixture was placed in a relative humidity (RH)-controlled chamber and soaked at a predefined RH until equilibrium was reached. RH was varied stepwise in a cyclic mode, while the change in film resistance was measured *in situ*, using a high-resistance digital multimeter (6517B, Keithley Instruments) at an applied voltage of 3 V.

Conflict of Interest: The authors declare no competing financial interest.

Acknowledgment. This work was supported by a grant (Code No. 2011-0031630) from the Center for Advanced Soft Electronics under the Global Frontier Research Program through the National Research Foundation (NRF) funded by the Ministry of Science, ICT and Future Planning (MSIE), Korea. Additional support was provided by the Ministry of Education (MOE) and NRF through the BK21 Plus Program (META-material-based Energy Harvest and Storage Technologies, 10Z20130011057) and the Human Resource Training Project for Regional Innovation (No. 2012H1B8A2026133).

Supporting Information Available: Additional characterization data from XPS and SEM, and the experimental setup for humidity sensing. This material is available free of charge *via* the Internet at http://pubs.acs.org.

REFERENCES AND NOTES

1. Breuer, O.; Sundararaj, U. Big Returns from Small Fibers: A Review of Polymer/Carbon Nanotube Composites. *Polym. Compos.* **2004**, *25*, 630–645.
2. Hussain, F.; Hojjati, M.; Okamoto, M.; Gorga, R. E. Review Article: Polymer-Matrix Nanocomposites, Processing, Manufacturing, and Application: An Overview. *J. Compos. Mater.* **2006**, *40*, 1511–1575.
3. Kuilla, T.; Bhadra, S.; Yao, D.; Kim, N. H.; Bose, S.; Lee, J. H. Recent Advances in Graphene Based Polymer Composites. *Prog. Polym. Sci.* **2010**, *35*, 1350–1375.
4. Novoselov, K. S.; Geim, A. K.; Morozov, S. V.; Jiang, D.; Zhang, Y.; Dubonos, S. V.; Grigorieva, I. V.; Firsov, A. A. Electric Field Effect in Atomically Thin Carbon Films. *Science* **2004**, *306*, 666–669.
5. Dikin, D. A.; Stankovich, S.; Zimney, E. J.; Piner, R. D.; Dommett, G. H. B.; Evmenenko, G.; Nguyen, S. T.; Ruoff, R. S. Preparation and Characterization of Graphene Oxide Paper. *Nature* **2007**, *448*, 457–460.
6. Avouris, P.; Chen, Z.; Perebeinos, V. Carbon-Based Electronics. *Nat. Nanotechnol.* **2007**, *2*, 605–615.
7. Kotov, N. A. Materials Science: Carbon Sheet Solutions. *Nature* **2006**, *442*, 254–255.
8. Huang, X.; Qi, X.; Boey, F.; Zhang, H. Graphene-Based Composites. *Chem. Soc. Rev.* **2012**, *41*, 666–686.
9. Stankovich, S.; Dikin, D. A.; Dommett, G. H. B.; Kohlhaas, K. M.; Zimney, E. J.; Stach, E. A.; Piner, R. D.; Nguyen, S. T.; Ruoff, R. S. Graphene-Based Composite Materials. *Nature* **2006**, *442*, 282–286.
10. Boukhvalov, D. W.; Katsnelson, M. I. Chemical Functionalization of Graphene. *J. Phys.: Condens. Matter* **2009**, *21*, 344205.
11. Green, A. A.; Hersam, M. C. Solution Phase Production of Graphene with Controlled Thickness *via* Density Differentiation. *Nano Lett.* **2009**, *9*, 4031–4036.
12. Chen, D.; Feng, H.; Li, J. Graphene Oxide: Preparation, Functionalization, and Electrochemical Applications. *Chem. Rev.* **2012**, *112*, 6027–6053.
13. Kim, J.; Cote, L. J.; Kim, F.; Yuan, W.; Shull, K. R.; Huang, J. Graphene Oxide Sheets at Interfaces. *J. Am. Chem. Soc.* **2010**, *132*, 8180–8186.
14. Tang, L.; Li, X.; Ji, R.; Teng, K. S.; Tai, G.; Ye, J.; Wei, C.; Lau, S. P. Bottom-up Synthesis of Large-Scale Graphene Oxide Nanosheets. *J. Mater. Chem.* **2012**, *22*, 5676–5683.
15. Sahoo, N. G.; Rana, S.; Cho, J. W.; Li, L.; Chan, S. H. Polymer Nanocomposites Based on Functionalized Carbon Nanotubes. *Prog. Polym. Sci.* **2010**, *35*, 837–867.
16. Zhao, J.; Morgan, A. B.; Harris, J. D. Rheological Characterization of Polystyrene–Clay Nanocomposites to Compare the Degree of Exfoliation and Dispersion. *Polymer* **2005**, *46*, 8641–8660.
17. Song, Y. S.; Youn, J. R. Influence of Dispersion States of Carbon Nanotubes on Physical Properties of Epoxy Nanocomposites. *Carbon* **2005**, *43*, 1378–1385.
18. Gojny, F. H.; Wichmann, M. H. G.; Köpke, U.; Fiedler, B.; Schulte, K. Carbon Nanotube-Reinforced Epoxy-Composites: Enhanced Stiffness and Fracture Toughness at Low Nanotube Content. *Compos. Sci. Technol.* **2004**, *64*, 2363–2371.
19. Yasmin, A.; Luo, J.-J.; Daniel, I. M. Processing of Expanded Graphite Reinforced Polymer Nanocomposites. *Compos. Sci. Technol.* **2006**, *66*, 1182–1189.
20. Zheng, W.; Wong, S.-C. Electrical Conductivity and Dielectric Properties of Pmma/Expanded Graphite Composites. *Compos. Sci. Technol.* **2003**, *63*, 225–235.
21. Wang, W.-p.; Liu, Y.; Li, X.-x.; You, Y.-z. Synthesis and Characteristics of Poly(Methyl Methacrylate)/Expanded Graphite Nanocomposites. *J. Appl. Polym. Sci.* **2006**, *100*, 1427–1431.
22. Kalaitzidou, K.; Fukushima, H.; Drzal, L. T. A New Compounding Method for Exfoliated Graphite–Polypropylene Nanocomposites with Enhanced Flexural Properties and Lower Percolation Threshold. *Compos. Sci. Technol.* **2007**, *67*, 2045–2051.
23. Kalaitzidou, K.; Fukushima, H.; Drzal, L. T. Mechanical Properties and Morphological Characterization of Exfoliated Graphite–Polypropylene Nanocomposites. *Compos. Part A* **2007**, *38*, 1675–1682.
24. Wakabayashi, K.; Pierre, C.; Dikin, D. A.; Ruoff, R. S.; Ramanathan, T.; Brinson, L. C.; Torkelson, J. M. Polymer–Graphite Nanocomposites: Effective Dispersion and Major Property Enhancement *via* Solid-State Shear Pulverization. *Macromolecules* **2008**, *41*, 1905–1908.
25. Pan, Y.-X.; Yu, Z.-Z.; Ou, Y.-C.; Hu, G.-H. A New Process of Fabricating Electrically Conducting Nylon 6/Graphite Nanocomposites *via* Intercalation Polymerization. *J. Polym. Sci., Part B: Polym. Phys.* **2000**, *38*, 1626–1633.
26. Ramanathan, T.; Abdala, A. A.; Stankovich, S.; Dikin, D. A.; Herrera Alonso, M.; Piner, R. D.; Adamson, D. H.; Schniepp, H. C.; Chen, X.; Ruoff, R. S.; Nguyen, S. T.; Aksay, I. A.; Prud'Homme, R. K.; Brinson, L. C. Functionalized Graphene Sheets for Polymer Nanocomposites. *Nat. Nanotechnol.* **2008**, *3*, 327–331.
27. Zhang, L.; Wang, Z.; Xu, C.; Li, Y.; Gao, J.; Wang, W.; Liu, Y. High Strength Graphene Oxide/Polyvinyl Alcohol Composite Hydrogels. *J. Mater. Chem.* **2011**, *21*, 10399–10406.
28. Wang, J.; Wang, X.; Xu, C.; Zhang, M.; Shang, X. Preparation of Graphene/Poly(Vinyl Alcohol) Nanocomposites with Enhanced Mechanical Properties and Water Resistance. *Polym. Int.* **2011**, *60*, 816–822.
29. Lee, H.; Dellatore, S. M.; Miller, W. M.; Messersmith, P. B. Mussel-Inspired Surface Chemistry for Multifunctional Coatings. *Science* **2007**, *318*, 426–430.
30. Lee, H.; Scherer, N. F.; Messersmith, P. B. Single-Molecule Mechanics of Mussel Adhesion. *Proc. Natl. Acad. Sci. U. S. A.* **2006**, *103*, 12999–13003.
31. Yang, L.; Phua, S. L.; Teo, J. K. H.; Toh, C. L.; Lau, S. K.; Ma, J.; Lu, X. A Biomimetic Approach to Enhancing Interfacial Interactions: Polydopamine-Coated Clay as Reinforcement for Epoxy Resin. *ACS Appl. Mater. Interfaces* **2011**, *3*, 3026–3032.
32. Kang, S. M.; Park, S.; Kim, D.; Park, S. Y.; Ruoff, R. S.; Lee, H. Simultaneous Reduction and Surface Functionalization of Graphene Oxide by Mussel-Inspired Chemistry. *Adv. Funct. Mater.* **2011**, *21*, 108–112.
33. Shin, M.; Kim, H. K.; Lee, H. Dopamine-Loaded Poly-(D,L-Lactic-Co-Glycolic Acid) Microspheres:New Strategy for Encapsulating Small Hydrophilic Drugs with High Efficiency. *Biotechnol. Prog.* **2014**, *30*, 215–223.
34. Ryu, S.; Lee, Y.; Hwang, J.-W.; Hong, S.; Kim, C.; Park, T. G.; Lee, H.; Hong, S. H. High-Strength Carbon Nanotube Fibers Fabricated by Infiltration and Curing of Mussel-Inspired Catecholamine Polymer. *Adv. Mater.* **2011**, *23*, 1971–1975.
35. Li, D.; Muller, M. B.; Gilje, S.; Kaner, R. B.; Wallace, G. G. Processable Aqueous Dispersions of Graphene Nanosheets. *Nat. Nanotechnol.* **2008**, *3*, 101–105.
36. Yamaguchi, H.; Eda, G.; Mattevi, C.; Kim, H.; Chhowalla, M. Highly Uniform 300 mm Wafer-Scale Deposition of Single and Multilayered Chemically Derived Graphene Thin Films. *ACS Nano* **2010**, *4*, 524–528.
37. d'Ischia, M.; Napolitano, A.; Pezzella, A.; Meredith, P.; Sarna, T. Chemical and Structural Diversity in Eumelanins: Unexplored Bio-Optoelectronic Materials. *Angew. Chem., Int. Ed.* **2009**, *48*, 3914–3921.
38. Dreyer, D. R.; Miller, D. J.; Freeman, B. D.; Paul, D. R.; Bielawski, C. W. Elucidating the Structure of Poly(Dopamine). *Langmuir* **2012**, *28*, 6428–6435.
39. Guo, L.; Liu, Q.; Li, G.; Shi, J.; Liu, J.; Wang, T.; Jiang, G. A Mussel-Inspired Polydopamine Coating as a Versatile Platform for the *In Situ* Synthesis of Graphene-Based Nanocomposites. *Nanoscale* **2012**, *4*, 5864–5867.
40. Kong, J.; Yee, W. A.; Yang, L.; Wei, Y.; Phua, S. L.; Ong, H. G.; Ang, J. M.; Li, X.; Lu, X. Highly Electrically Conductive Layered Carbon Derived from Polydopamine and Its Functions in Sno2-Based Lithium Ion Battery Anodes. *Chem. Commun.* **2012**, *48*, 10316–10318.
41. Kang, S. M.; Park, S.; Kim, D.; Park, S. Y.; Ruoff, R. S.; Lee, H. Simultaneous Reduction and Surface Functionalization of Graphene Oxide by Mussel-Inspired Chemistry. *Adv. Funct. Mater.* **2011**, *21*, 108–112.
42. Paredes, J. I.; Villar-Rodil, S.; Martínez-Alonso, A.; Tascón, J. M. D. Graphene Oxide Dispersions in Organic Solvents. *Langmuir* **2008**, *24*, 10560–10564.

43. Centeno, S. A.; Shamir, J. Surface Enhanced Raman Scattering (Sers) and Ftir Characterization of the Sepia Melanin Pigment Used in Works of Art. *J. Mol. Struct.* **2008**, *873*, 149–159.
44. Zhao, X.; Zhang, Q.; Chen, D.; Lu, P. Enhanced Mechanical Properties of Graphene-Based Poly(Vinyl Alcohol) Composites. *Macromolecules* **2010**, *43*, 2357–2363.
45. Wang, H.; Feng, C.-D.; Sun, S.-L.; Segre, C. U.; Stetter, J. R. Comparison of Conductometric Humidity-Sensing Polymers. *Sens. Actuators, B* **1997**, *40*, 211–216.
46. Li, Y.; Ying, B.; Hong, L.; Yang, M. Water-Soluble Polyaniline and Its Composite with Poly(Vinyl Alcohol) for Humidity Sensing. *Synth. Met.* **2010**, *160*, 455–461.
47. Fuke, M. V.; Adhyapak, P. V.; Mulik, U. P.; Amalnerkar, D. P.; Aiyer, R. C. Electrical and Humidity Characterization of M-Na Doped Au/Pva Nanocomposites. *Talanta* **2009**, *78*, 590–595.
48. Barkauskas, J. Investigation of Conductometric Humidity Sensors. *Talanta* **1997**, *44*, 1107–1112.
49. Yang, M.-R.; Chen, K.-S. Humidity Sensors Using Polyvinyl Alcohol Mixed with Electrolytes. *Sens. Actuators, B* **1998**, *49*, 240–247.